Quantum Dot Nano Thermometers Reveal Heterogeneous Local Thermogenesis in Living Cells

Jui-Ming Yang,[†] Haw Yang,[‡,§,*] and Liwei Lin[†,*]

[†]Berkeley Sensor and Actuator Center, Department of Mechanical Engineering, University of California at Berkeley, Berkeley California 94720, United States, [‡]Department of Chemistry, University of California at Berkeley, and Physical Biosciences Division, Lawrence Berkeley National Laboratory, Berkeley California 94720, United States, and [§]Department of Chemistry, Princeton University, Princeton, New Jersey 08544, United States

ABSTRACT The local temperature response inside single living cells upon external chemical and physical stimuli was characterized using quantum dots as nano thermometers. The photoluminescence spectral shifts from endocytosed quantum dots were used to map intracellular heat generation in NIH/3T3 cells following Ca^{2+} stress and cold shock. The direct observation of inhomogeneous intracellular temperature progression raises interesting new possibilities, including further innovations in nanomaterials for sensing local responses, as well as the concept of subcellular temperature gradient for signaling and regulation in cells.

KEYWORDS: thermal signaling · intracellular temperature · spectral imaging · single-cell analysis · nanobio

Myriads of biochemical reactions take place in the complex, compartmentalized cellular environment, creating and maintaining concentration gradients and releasing free energy to drive a variety of cellular activities. Unutilized energy is discharged as heat, which in principle will result in elevated local temperature. Cells can also generate heat purposely; in this regard, mitochondria have long been recognized as the chief intracellular organelle for thermogenesis.[1,2] Mitochondria also play a central role in orchestrating diverse cellular processes including energy metabolism[3] and programmed cell death (apoptosis).[4] Raising the local temperature not only accelerates kinetic rates and shifts chemical equilibria, but also alters the physical state of DNA and proteins,[5] as well of other biomaterials. Considering the complexity of the intracellular environment, the local temperature progression is likely to be heterogeneous. This picture, however, has hitherto not been experimentally established.

Several approaches have been proposed to detect cellular temperature response using the emission intensity or lifetime of organic dyes[6,7] and transition-metal ions.[8,9] These pioneering works were able to provide the average temperature for individual cells. Compared to organic dyes, quantum dots exhibit superior brightness for detection, a broader excitation profile for multiplexing, and better photostability for long-term studies.[10−12] Furthermore, quantum dots as temperature sensors are resistant to pH and other environmental variations that are expected to be prevalent inside a cell. The spectroscopic characteristics of quantum dots have been shown to be a strong function of temperature both at the bulk[13] and at the single-particle[14] levels. At elevated temperatures, for CdSe nanocrystals, the lattice becomes dilated, which in turn alters the electron−lattice interaction to result in a red-shifted emission spectrum.[15] The nanometer size of a quantum dot ensures a rapid thermal equilibrium with its environment—an important characteristic for time-dependent studies. Since our preliminary disclosure of the use of quantum dots for intracellular trmperature sensing,[16] Maestro *et al*. have reported the characterization of quantum dot spectral shifts in cells under two-photon excitation,[17] whereas Vitrone *et al*. have used Er/Yb-doped nanocrystals to look at intracellular temperature in HeLa cells with the pump−probe up-conversion technique.[18] In this work, we present the complete experiment and analysis for the time-dependent response of localized intracellular temperature for prolonged periods following the chemical calcium stress and the physical cold shock, reporting the first experimental evidence

* Address correspondence to hawyang@princeton.edu, lwlin@me.berkeley.edu.

Received for review March 26, 2011 and accepted May 16, 2011.

Published online May 16, 2011
10.1021/nn201142f

for the inhomogeneous local temperature progression in cells.

RESULTS AND DISCUSSION

Quantum dots with a central emission wavelength at ~655 nm were delivered into NIH/3T3 murine fibroblast cells using a commercially available QTracker cell labeling kit. Since the internalized quantum dots took up negligible volume fraction of a cell, their contribution to the heat transfer process could be omitted. The sample was mounted on an inverted microscope (Figure 1a). The experimental setup reported here used a 20× objective lens to give a spatial resolution of ~700 nm per pixel, constrained by the far-field optics diffraction. It should be noted that our approach in principle could attain a resolution beyond optical diffraction using off-line centroid fitting[19] with proper antibunching photon statistics taken into account,[20] limited only by the size of a single quantum dot (~20 nm).[21] A typical fluorescence image overlaid with a bright-field optical transmission micrograph is displayed in Figure 1b, where the width of the observation window was controlled by the entrance slit opening of the spectrometer (set to 100 μm). The relatively wide slit width permitted a prolonged study before the quantum dots moved out of observation window.

We first investigated chemically induced thermogenesis in single living cells. Ca^{2+} shock was used to boost heat production,[9] possibly by promoting the activities of ion pumps and accelerating the respiration rates.[22,23] NIH/3T3 cells were incubated in standard culture media with a Ca^{2+} concentration of ~10−100 nM. Two minutes into each single-cell experiment, ionomycin calcium complex (~1 μM) was added to elevate the intracellular concentration of Ca^{2+}. Figure 2a displays a representative position-spectral image snapshot, where the red dots represent automatically detected and localized quantum dots. Similar analyses were performed for subsequent frames, and the quantum dots spots in a sequence of frames were correlated using a software-based tracking algorithm (Supporting Information). The spectrum from each quantum dots spot along a correlated time trace was analyzed and compared with the spectrum of the first time points to extract the temperature shifts using the previously published calibration parameter,[14] $\Delta\lambda/\Delta T$ = 0.105 nm/°C. The position-dependent temperature changes for the data set shown in Figure 2a are displayed in Figure 2b. It is apparent that the temperature inside the cell rose following the addition of Ca^{2+} and that different regions of the cell exhibit different temperature progressions (*cf.* Figure 2d). Figure 2b also indicates that while most of the quantum dots did not move significantly during the experiment, some did travel over an appreciable distance especially

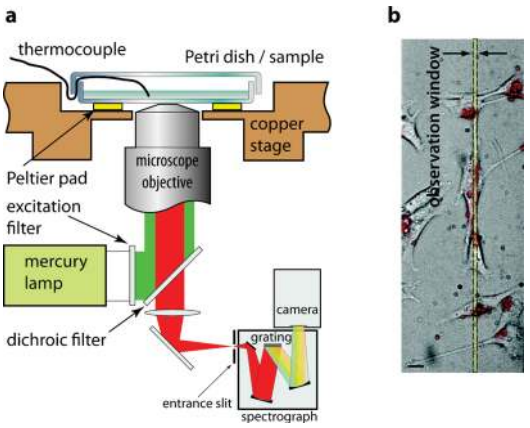

Figure 1. Experimental outline. (a) Schematic of the experimental setup, illustrating the essential optical pathways in an inverted microscope. (b) A bright-field optical transmission micrograph of cells overlaid with quantum dots emission image, shown in red. The dashed vertical lines indicate experimental observation window as determined by the slit width (~100 μm) of the monochromator. With a 20× objective lens, the observable region of the sample is ~5 μm. The scale bar at the bottom left is ~20 μm.

following the Ca^{2+} shock. The quantum dot movements were attributed to the diffusion and innate cellular activities, where the latter is expected to amplify significantly upon addition of calcium ions. To ensure that the observed spectral red-shift was indeed due to an increase in temperature rather than chemical modifications of the CdSe core by the Ca^{2+} shock, controls were carried out to repeat the same procedure but on fixed cells (see Supporting Information for other controls, including pH and illumination power). The results from four fixed cells are displayed in the inset of Figure 2d, which shows clearly that the intracellular temperature of fixed cells remained unchanged upon addition of Ca^{2+}. Taken together, these data suggest that the observed nonuniform temperature rise upon Ca^{2+} shock is correlated with the physiological responses of a living cell.

A population-level analysis of the temperature change was carried out. Figure 2c shows the ΔT distributions before (green) and after (red) Ca^{2+} shock combining all 31 cells examined with $\overline{\Delta T}_{Ca^{2+}}^{before\ shock}$ = −0.14 ± 0.15 °C and $\overline{\Delta T}_{Ca^{2+}}^{after\ shock}$ = +1.84 ± 0.27 °C, respectively. Importantly, the apparent temperature distribution after Ca^{2+} shock, $\hat{\sigma}(\Delta T_{Ca^{2+}}^{after\ shock})$ = 2.9 °C, was found to be much broader compared to the distribution before Ca^{2+} addition $\hat{\sigma}(\Delta T_{Ca^{2+}}^{before\ shock})$ = 1.6 (p-value = 10^{-15}). One notices on the distribution that some of the measurements extended to negative temperature change. Of the total 31 live cells examined, seven (23%) showed a decrease of average cellular temperature, seven (23%) showed no significant temperature change, and 17 (54%) showed a temperature rise. The apparent negative temperature response could be attributed to spectral readout errors resulting from extensive translocation of quantum dots

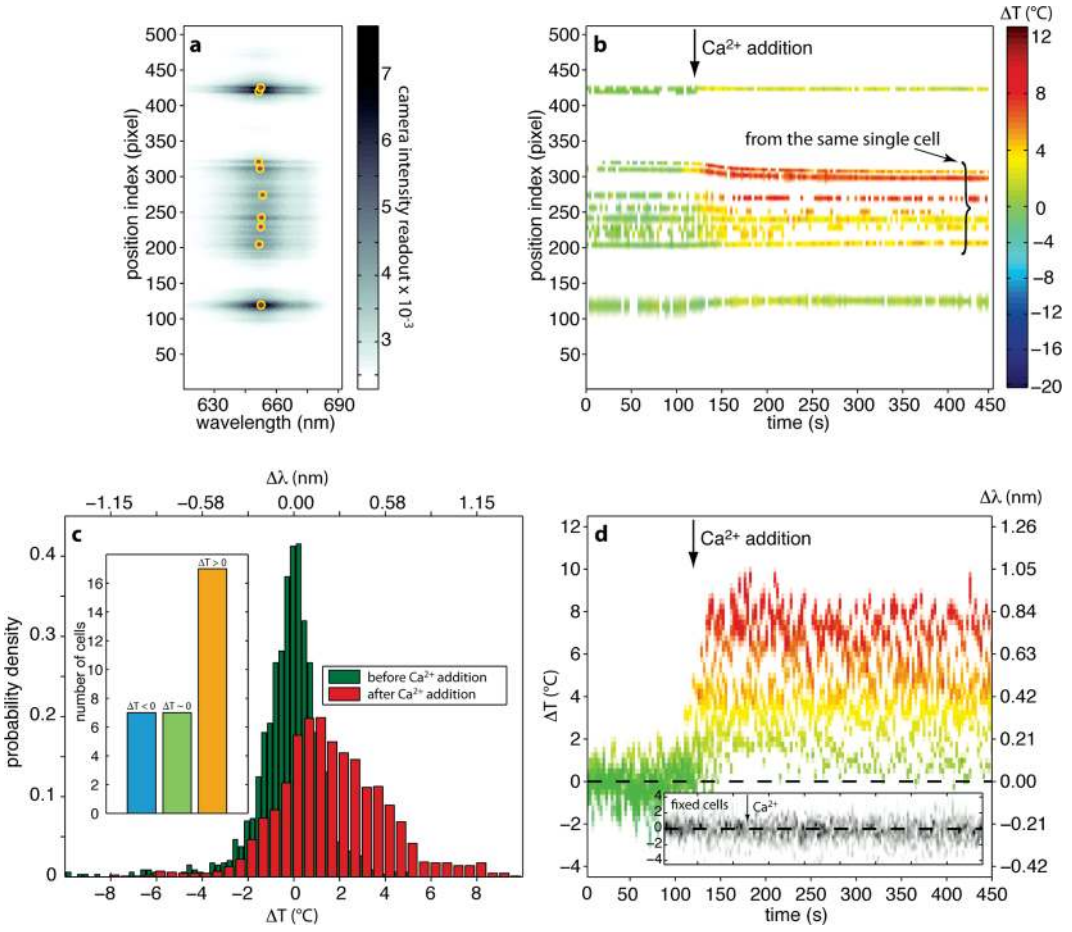

Figure 2. Chemical perturbation: Ca^{2+} shock experiments. (a) Representative snapshot of the raw position-spectrum maps for the sample shown in Figure 1b. The ordinate is the quantum dot position index in units of camera pixels, and the abscissa is the spectral index in units of pixels (0.144 nm/pixel). The positions of quantum dots were automatically detected and marked by red dots enclosed by yellow circles. The position and wavelength of each quantum dot spot were then determined by fitting the spectrum to a two-dimensional Gaussian profile. (b) Location-dependent intracellular temperature progression as a function of time of the same cell shown in (a). The time point at which ionomycin calcium complex was added, ~120 s, is marked by an arrow. The uncertainties of position localization as estimated from the Gaussian fitting are represented as shades of the temperature color; the more intense and the narrower the vertical distribution, the more accurately the location is. Note the nonlinear spacing in the color code for temperature shift. The same color code and scaling will be used for the remainder of this report for consistency. (c) Statistics of temperature shift for the 31 cells examined, showing significant broadening of the temperature shift distribution. Here, temperature shifts acquired between 30 and 100 s were categorized as "before Ca^{2+} addition", whereas those acquired between 350 and 450 s were categorized as "after Ca^{2+} addition". Inset: Cell-by-cell variations in temperature response to Ca^{2+} shock, showing that the majority of the cells exhibited increased temperature. (d) Local temperature shift as a function of time for the cell shown in (a) and (b), showing heterogeneous temperature response following Ca^{2+} shock. The uncertainties of the temperature measurement as estimated from the Gaussian fitting are represented as shades of the temperature color; the more intense and the narrower the vertical distribution, the more accurately the measurement is. Inset: Time-dependent local temperature shift of fixed cells, showing that no detectable temperature response upon addition of Ca^{2+}.

($\delta(\Delta T)_{QDmovement} \approx 2$ °C), which were not sufficiently compensated for by image-based tracking (see Supporting Information for error analysis). While the absolute temperature readout, including the magnitude of single-spot temperature shift measurements, could not yet be ascertained with high confidence using the current level of technology, these results provide direct evidence for inhomogeneous temperature response to Ca^{2+}-shock-induced thermogenesis inside individual live cells.

To further illustrate the quantum-dots nano thermometer capability, we developed a cold-shock assay to investigate subcellular temperature responses to abiotic stress. The ambient temperature of the cells was precipitously lowered from 37 to 15 °C using a home-built Peltier thermoelectric cooling device (*cf.* Figure 1a), and the intracellular temperature changes were recorded for 15 min, during which time the Peltier temperature was kept at 15 °C. The transient and position-dependent temperature progression trajectories in a typical cell are displayed in Figure 3a, in which temperature changes are coded in color. As observed in Figure 3a, the extent of quantum dot movements in cold-shock experiments was far less

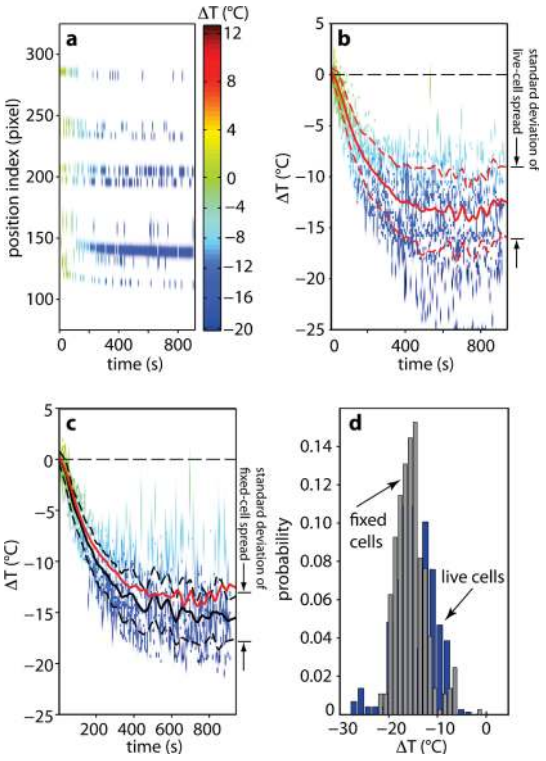

Figure 3. Physical perturbation: cold-shock experiments. (a) Position-dependent intracellular temperature progression as a function of time. Cold shock was turned on at $t = 0$. The uncertainties of position localization as estimated from the Gaussian fitting are represented as shades of the temperature color; the more intense and the narrower the vertical distribution, the more accurately the location is, and *vice versa*. (b) Local temperature shift after cold shock as a function of time accumulated over a total of 13 live cells. The uncertainties of temperature measurement as estimated from the Gaussian fitting are represented as shades of the temperature color; the more intense and the narrower the vertical distribution, the more accurately the measurement is, and *vice versa*. The thick solid and the dashed lines in red mark the mean and the standard deviation of the temperature progression distribution, respectively, and serve as an eye guide. (c) Analogous to (b) but with exactly the same 13 cells fixed *in situ*. The thick solid and the dashed lines in black are the mean and the standard deviation of the temperature shift spread at each time point and serve as an eye guide. To assist in visual comparison with (b), the mean temperature progression from (b) is reproduced here as the thick solid red line. The comparison suggests that on average the live cells exhibit a shallower cooling curve upon cold shock compared to fixed cells. (d) Statistics of cold-shock response for the live and fixed cells, showing significant broadening of the temperature shift distribution in live cells. Here, temperature shifts acquired between 600 and 900 s were included in the statistical analysis.

significant compared to that observed in Ca^{2+}-shock studies (Supporting Information). Using the same color-coding scheme, the local temperature progressions following cold shock for 13 cells are displayed in Figure 3b (live) and Figure 3c (fixed). In both cases, the intracellular temperature decreased, as expected, and reached a steady-state temperature after ~400 s. A visual inspection of these two plots suggests that, compared to fixed cells, live cells follow a shallower cooling curve and reach a slightly higher steady-state temperature with $\overline{\Delta T}^{\text{live cell}}_{\text{cold shock}} = -14.8 \pm 0.51$ °C and $\overline{\Delta T}^{\text{fixed cell}}_{\text{cold shock}} = -15.3 \pm 0.41$ °C. Akin to Le Châtelier's principle in chemical equilibrium, the live cells in the cold-shock experiments exhibited a predisposition to resist an abrupt shift to a colder environment, possibly by activating uncoupling pathways that promote heat generation.[24−26] Additionally, the apparent temperature progression in live cells was more broadly distributed (p-value = 2.5×10^{-10}) with $\hat{\sigma}(\Delta T^{\text{live cell}}_{\text{cold shock}}) = 4.48$ °C compared to fixed cells with $\hat{\sigma}(\Delta T^{\text{fixed cell}}_{\text{cold shock}}) = 3.09$ °C. In this set of cold-shock experiments, as a control, the cell on which the cold-shock studies were performed was killed and fixed *in situ*. Then additional series of cold-shock experiments were repeated on the same cell. Hence, it is not likely that the observed broader temperature distribution in live cells was a result of different locations of quantum dot sensors in different cells. These results, summarized in Figure 3d, therefore further reinforce the concept of transient inhomogeneous intracellular temperature response, but in the context of a cold-shock physical perturbation.

CONCLUSION

There is no known mechanism for a cell to actively dissipate excessive thermal energy; diffusion and possibly convection[27] are the primary means to passively remove the heat generated inside the cell. As such, highly localized heat sources are expected to create a subcellular temperature gradient. The direct observation of local heterogeneous temperature progression presented here substantiates such a concept. While micrometer- and nanoscale temperature gradients have been shown to influence the development of drosophila embryos[28] and locally activate temperature-sensitive ion channels in *Caenorhabditis elegans*,[29] respectively, it is now possible to put forward the hypothesis that individual cells may also utilize a transient thermal gradient for signaling with the demonstrated technique of quantum-dots nano thermometers.

METHODS

The details of the experimental approach and discussion are described in the Supporting Information. Briefly, streptavidin-coated quantum dots (QD655) were purchased from QDots/Invitrogen and used as received. The NIH/3T3 murine fibroblast cells were purchased from the American Type Culture Collection, CRL-1658, and cultured in a glass-bottom Petri dish with high-glucose Dulbecco's modified Eagle medium (DMEM) containing 10% bovine serum with antibiotic mixture. The Ca^{2+}-shock and cold-shock experiments were conducted when cells were at about 40% confluence. The time-lapsed digital images were analyzed using a set of scripts written in MATLAB, making

use of the standard library such as wavelet denoising and automated spot finding. To take into account movements of the image spots, we have also developed new model-free tracking algorithms based on ideas in applied statistics and information theory. The results of the model-free tracking algorithm were refined by cross validation. The uncertainties, accumulated from the raw data according to the usual error propagation rules, were used to assess the confidence level of the cellular thermogensis analysis, quantified by the *p*-value statistics. Only statistically significant observations were reported and discussed.

Acknowledgment. We acknowledge the Cancer Research Laboratory Molecular Imaging Center at the University of California, Berkeley, in which confocal images were generated. We thank H. Cang and K. Zhang for technical help with optical setup, as well as Q. Zhou, B. T. Nixon, and B. Sun for helpful discussions. This work was supported by National Science Foundation (to L.L.) and by the U.S. Department of Energy (to H.Y.).

Supporting Information Available: Experimental details including cell culture, quantum dot uptake, immunofluorescence staining, apparatus, image acquisition, Ca^{2+}-shock experiment, cold-shock experiment; analysis details including detection and localization of quantum dots in position-spectrum images, classification of quantum dot positions, cross validation of model-free quantum dot spot tracking, error bars, cell-by-cell temperature change, temperature progression distribution; exanded discussion including addition of quantum dots not altering thermal characteristics of a cell, steady-state measurements, spectral shifts indpendent of pH or illumination intensity, verification of intracellular Ca^{2+} increase upon addition of ionomycin calcium complex, cell viability tests, heat-transfer calculations, estimation of heat released; references. This material is available free of charge *via* the Internet at http://pubs.acs.org.

REFERENCES AND NOTES

1. Prusiner, S.; Poe, M. Thermodynamic Cosiderations of Mammalian Thermogenesis. *Nature* **1968**, *220*, 235–237.
2. Himms-Hagen, J. Cellular Thermogenesis. *Annu. Rev. Physiol.* **1976**, *38*, 315–351.
3. Dröge, W. Free Radicals in the Physiological Control of Cell Function. *Physiol. Rev.* **2002**, *82*, 47–95.
4. +Kroemer, G.; Galluzzi, L.; Brenner, C. Mitochondrial Membrane Permeabilization in Cell Death. *Physiol. Rev.* **2007**, *87*, 99–163.
5. Sanchez-Ruiz, J. M. Protein Kinetic Stability. *Biophys. Chem.* **2010**, *148*, 1–15.
6. Chapman, C. F.; Liu, Y.; Sonek, G. J.; Tromberg, B. J. The Use of Exogenous Fluorescent-Probes for Temperature-Measurements in Single Living Cells. *Photochem. Photobiol.* **1995**, *62*, 416–425.
7. Gota, C.; Okabe, K.; Funatsu, T.; Harada, Y.; Uchiyama, S. Hydrophilic Fluorescent Nanogel Thermometer for Intracellular Thermometry. *J. Am. Chem. Soc.* **2009**, *131*, 2766–2767.
8. Zohar, O.; Ikeda, M.; Shinagawa, H.; Inoue, H.; Nakamura, H.; Elbaum, D.; Alkon, D. L.; Yoshioka, T. Thermal Imaging of Receptor-Activated Heat Production in Single Cells. *Biophys. J.* **1998**, *74*, 82–89.
9. Suzuki, M.; Tseeb, V.; Oyama, K.; Ishiwata, S. Microscopic Detection of Thermogenesis in a Single HeLa Cell. *Biophys. J.* **2007**, *92*, L46–L48.
10. Jamieson, T.; Bakhshi, R.; Petrova, D.; Pocock, R.; Imani, M.; Seifalian, A. M. Biological Applications of Quantum Dots. *Biomaterials* **2007**, *28*, 4717–4732.
11. Smith, A. M.; Duan, H. W.; Mohs, A. M.; Nie, S. M. Bioconjugated Quantum Dots for in vivo Molecular and Cellular Imaging. *Adv. Drug Delivery Rev.* **2008**, *60*, 1226–1240.
12. Resch-Genger, U.; Grabolle, M.; Cavaliere-Jaricot, S.; Nitschke, R.; Nann, T. Quantum Dots Versus Organic Dyes as Fluorescent Labels. *Nat. Methods* **2008**, *5*, 763–775.
13. Walker, G. W.; Sundar, V. C.; Rudzinski, C. M.; Wun, A. W.; Bawendi, M. G.; Nocera, D. G. Quantum-Dot Optical Temperature Probes. *Appl. Phys. Lett.* **2003**, *83*, 3555–3557.
14. Li, S.; Zhang, K.; Yang, J. M.; Lin, L. W.; Yang, H. Single Quantum Dots as Local Temperature Markers. *Nano Lett.* **2007**, *7*, 3102–3105.
15. Varshni, Y. P. Temperature Dependence of Energy Gap in Semiconductors. *Physica* **1967**, *34*, 149–154.
16. Yang, J.-M.; Yang, H.; Lin, L. Thermogenesis Detection of Single Living Cells via Quantum Dots. In *The 23rd IEEE Micro Electro Mechanical Systems Conference*, Hong Kong, 2010; pp 963−966.
17. Maestro, L. M.; Rodríguez, E. M.; Rodríguez, F. S.; Iglesias-de la Cruz, M. C.; Juarranz, A.; Naccache, R.; Vetrone, F.; Jaque, D.; Capobianco, J. A.; Solé, J. G. CdSe Quantum Dots for Two-Photon Fluorescence Thermal Imaging. *Nano Lett.* **2010**, *10*, 5109–5115.
18. Vetrone, F.; Naccache, R.; Zamarron, A.; de la Fuente, A. J.; Sanz-Rodriguez, F.; Maestro, L. M.; Rodriguez, E. M.; Jaque, D.; Sole, J. G.; Capobianco, J. A. Temperature Sensing Using Fluorescent Nanothermometers. *ACS Nano* **2010**, *4*, 3254–3258.
19. Lidke, K. A.; Rieger, B.; Jovin, T. M.; Heintzmann, R. Superresolution by Localization of Quantum Dots Using Blinking Statistics. *Opt. Express* **2005**, *13*, 7052–7062.
20. Nair, G.; Zhao, J.; Bawendi, M. G. Biexciton Quantum Yield of Single Semiconductor Nanocrystals from Photon Statistics. *Nano Lett.* **2011**, *11*, 1136–1140.
21. Ober, R. J.; Ram, S.; Ward, E. S. Localization Accuracy in Single-Molecule Microscopy. *Biophys. J.* **2004**, *86*, 1185–1200.
22. Engström, I.; Waldenström, A.; Nilssonehle, P.; Ronquist, G. Dissipation of the Calcium Gradient in Human Erythrocytes Results in Increased Heat-Production. *Clin. Chim. Acta* **1993**, *219*, 113–122.
23. de Meis, L.; Ketzer, L. A.; da Costa, R. M.; de Andrade, I. R.; Benchimol, M. Fusion of the Endoplasmic Reticulum and Mitochondrial Outer Membrane in Rats Brown Adipose Tissue: Activation of Thermogenesis by Ca^{2+}. *PLoS One* **2010**, 5.
24. Lowell, B. B.; Spiegelman, B. M. Towards a Molecular Understanding of Adaptive Thermogenesis. *Nature* **2000**, *404*, 652–660.
25. Toyomizu, M.; Ueda, M.; Sato, S.; Seki, Y.; Sato, K.; Akiba, Y. Cold-Induced Mitochondrial Uncoupling and Expression of Chicken UCP and ANT mRNA in Chicken Skeletal Muscle. *FEBS Lett.* **2002**, *529*, 313–318.
26. Wijers, S. L. J.; Schrauwen, P.; Saris, W. H. M.; Lichtenbelt, W. D. V. Human Skeletal Muscle Mitochondrial Uncoupling Is Associated with Cold Induced Adaptive Thermogenesis. *PLoS One* **2008**, 3.
27. Hochachka, P. W. Intracellular Convection, Homeostasis and Metabolic Regulation. *J. Exp. Biol.* **2003**, *206*, 2001–2009.
28. Lucchetta, E. M.; Lee, J. H.; Fu, L. A.; Patel, N. H.; Ismagilov, R. F. Dynamics of Drosophila Embryonic Patterning Network Perturbed in Space and Time Using Microfluidics. *Nature* **2005**, *434*, 1134–1138.
29. Huang, H.; Delikanli, S.; Zeng, H.; Ferkey, D. M.; Pralle, A. Remote Control of Ion Channels and Neurons Through Magnetic-Field Heating of Nanoparticles. *Nat. Nanotechnol.* **2010**, *5*, 602–606.